Solid-State NMR Characterization and Determination of the Orientational Order of a Nematogen

T. Narasimhaswamy,[†,‡] M. Monette,[§] D. K. Lee,[†,||] and A. Ramamoorthy*[,†]

Department of Chemistry and Biophysics Research Division, University of Michigan, Ann Arbor, Michigan 48109-1055, and Bruker BioSpin Ltd., Milton, Ontario L9T 1Y6, Canada

Received: May 5, 2005; In Final Form: August 13, 2005

Thermotropic liquid crystalline compounds are of considerable importance due to their potential applications as advanced functional materials. A mesogen consisting of a terminal dimethylamino group, which can act as a charge-transfer donor, is particularly valuable for its light emission and nonlinear optical properties. In this study, we report the solid-state NMR investigation of the nematic behavior of one such novel mesogen (4-(dodecyloxy)benzoic acid 4-[((4-(dimethylamino)phenyl)imino)methyl]phenyl ester). Static and MAS experiments were performed on nematic and crystalline phases of the compound to measure ^{13}C chemical shift, $^{13}C-^{1}H$ dipolar coupling, and ^{1}H chemical shift values. 2D chemical shift correlation of ^{1}H and ^{13}C nuclei confirmed the ^{13}C chemical shift values determined from 1D CPMAS experiments. The appearance of more peaks in both CPMAS and $^{13}C-^{1}H$ HETCOR spectra of a crystalline solid suggests the heterogeneous orientations of phenyl rings of the mesogenic core. Variable-temperature experiments infer the motional averaging of these orientations before melting. The $^{1}H-^{13}C$ dipolar coupling values, measured by 2D PITANSEMA experiments, were used to determine the orientational order of the mesogenic core at various temperatures. The influence of the linking unit and terminal substituents on the order parameter values of the mesogenic core is discussed.

Introduction

Supramolecular liquid crystals constitute noncovalent intermolecular forces such as hydrogen-bonding,[1,2] charge-transfer (CT), and $\pi-\pi$ interactions.[3−6] These interactions leading to the formation of a mesophase require either a mesogenic donor or an acceptor (complementary units). Much of the published work deals with the hydrogen-bonded liquid crystals, while studies on other noncovalent forces such as CT and $\pi-\pi$ interactions[3−7] are increasingly gaining importance. Intramolecular CT in dimethylamino compounds has attracted the interest of both quantum chemical[8,9] and experimental researchers mainly due to the unusual dual florescence exhibited by 4-(dimethylamino)benzonitrile and other systems.[11,12] Very recent studies demonstrated the utility of dimethylamino-based aromatic systems as advanced functional materials due to their nonlinear optical property for potential application in optoelectronics and photonics.[13,14] Therefore, designing a new class of materials containing a dimethylamino group with a liquid crystalline property could provide further opportunities to develop multifunctional molecules. One such class of systems containing a dimethylamino group as a mesogenic CT donor was recently reported,[15] even though dimethylamino is not a good terminal functional group.[16]

The molecular order in thermotropic liquid crystals is represented as positional and orientational depending on the nature of the phase.[17] While the orientational order is common for all the phases of calamitic mesogens, the positional order is only observed in smectic phases.[17] The measurement of the orientational order in nematic and other smectic phases is an important aspect in understanding the dynamics of the phase. The long-range orientational order is the characteristic property of a nematic phase which distinguishes it from the isotropic phase. This characteristic property of mesogens is typically measured using a variety of physical techniques such as optical birefringence and infrared, Raman, X-ray, and dielectric spectroscopy.[18] However, high-resolution solid-state NMR spectroscopy is one of the most powerful spectroscopic tools for probing atomistic-level details of anisotropic fluids.[19] In recent years, this technique has become popular for characterizing various aspects of all classes of thermotropic liquid crystals.[20−22] The natural abundance ^{13}C static and MAS experiments can provide information about the molecular structure in both the solid phase and the mesophase. Experimentally measured chemical shifts and heteronuclear dipole−dipole interactions can provide information on the ordering of various fragments of the mesogens.[23−25] It can differentiate the ordering of the core unit from that of the aliphatic tail and even within the core unit of the compound.[26,27] Measurement of the ordering of phenyl rings and linking units is also possible using solid-state NMR, while such measurements are not possible with other physical techniques. Moreover, probing the segmental ordering of mesogens would be useful in understanding the role of each segment (both at the core and in terminal units) in deciding the molecular anisotropy. This information can also be used in designing novel structures with more exotic liquid crystalline materials for future functional materials. This work deals with the detailed characterization of the molecular structure of a novel mesogen, DoBDPMP (4-(dodecyloxy)benzoic acid 4-[((4-(di-

* To whom correspondence should be addressed. Phone: (734) 647-6572. Fax: (734) 763-2307. E.mail: ramamoor@umich.edu.

† University of Michigan.

‡ Present address: Polymer Laboratory, Central Leather Research Institute, Adayaru, Chennai, Tamil Nadu, India.

§ Bruker BioSpin Ltd.

|| Present address: Department of Fine Chemistry, Seoul National University of Technology, Seoul, Korea 139-743.

10.1021/jp052343v CCC: $30.25
Published on Web 09/24/2005

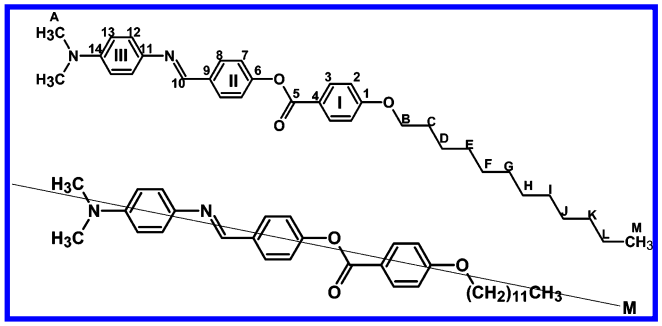

Figure 1. Molecular structure of a nematogen, DoBDPMP.

methylamino)phenyl)imino)methyl]phenyl ester), in solid, meso, and isotropic phases, and also the determination of the orientational order of the core fragment. This dimethyamino-containing nematogen is expected to retain its mesophase even in the presence of a nonmesogenic nitro- or cyano-substituted phenyl ring containing acceptor.

Experimental Section

The synthetic details of DoBDPMP are reported elsewhere.[15] The ^{13}C NMR spectrum was recorded in $CDCl_3$ solution on a Bruker 300 MHz spectrometer operating at a resonance frequency of 75.47 MHz for ^{13}C at room temperature using TMS as an internal standard. All solid-state NMR experiments were performed on a Varian Infinity 400 MHz spectrometer. Resonance frequencies of ^{13}C and ^{1}H nuclei were 100.65 and 400.14 MHz, respectively. A 5 mm Chemagnetics triple (HXY) resonance MAS probe and a 5 mm zirconia rotor were used. The sample was recrystallized from ethyl acetate and vacuum-dried before use. The ^{13}C CPMAS spectra were obtained using a 6 or 9 $\pm$ 0.001 kHz spinning speed, a ramp-cross-polarization pulse sequence,[28,29] a 2 ms contact time, a 75 kHz two-pulse phase modulation (TPPM) proton decoupling,[30] and a 3 s recycle delay. ^{13}C chemical shift frequencies are referenced to the peak for TMS by setting the observed ^{13}C signals of a solid adamantane to 29.5 and 38.56 ppm. Experimental data were processed in a Sun Sparc computer using the Spinsight software (Varian). A total of 2000 data points were zero-filled to 16000 points after apodization using a 50 Hz exponential line broadening. The temperature of the samples was maintained with an accuracy of 0.1 °C using a Varian temperature controller.

Results and Discussion

The molecular structure of the nematogen is shown in Figure 1. The compound exhibits an enantiotropic nematic phase as confirmed by a hot-stage polarizing microscope and differential scanning calorimetry.[15] The core of the mesogen consists of three phenyl rings and azomethine and ester linking units. The dodecyloxy unit is present in one terminal, and the other terminal consists of a dimethylamino group. The crystalline to nematic phase transition temperature (T_{CN}) of the nematogen is 146 °C, while the transition from the nematic to the isotropic phase (T_{NI}) occurs at 209.3 °C. A monotropic smectic A phase was also noticed at 107.1 °C.[15] As mentioned earlier, the dimethylamino group is not a good terminal functionality to observe a mesophase but a good charge-transfer donor. Therefore, very few liquid crystalline compounds containing a dimethylamino terminal group are reported in the literature.[31] In view of this, the core of the mesogen is designed to have three phenyl rings with azomethine and ester groups as linking units to enhance the molecular polarizability, which is reflected in the phase stability ($T_{NI} - T_{CN} = 63.3$ °C).

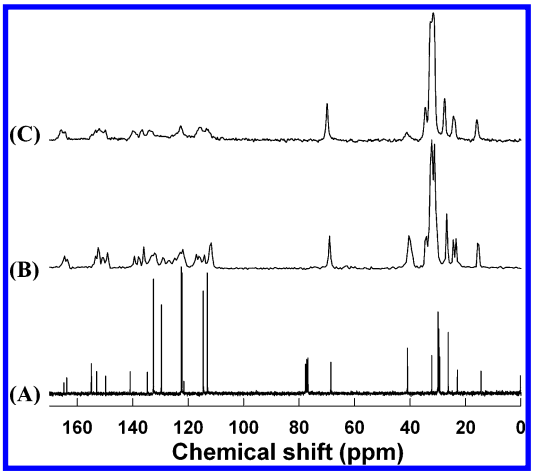

Figure 2. Carbon-13 isotropic chemical shift spectra of DoBDPMP: (A) solution at 23 °C; (B) 9 kHz MAS at 23 °C; (C) 8.5 kHz MAS at 100 °C. Spectra A, B, and C were obtained using 1000, 2020, and 2616 scans, respectively.

^{13}C Spectrum of the DoBDPMP Solution. The purity and identity of the compound was checked using natural abundance ^{13}C solution NMR spectroscopy. A ^{13}C spectrum of DoBDPMP in $CDCl_3$ solution is given in Figure 2A. The region 100−165 ppm in the solution spectrum (Figure 2A) accounts for the core fragment of the mesogen, and the peaks are mainly from phenyl ring carbons and linking units such as azomethine and ester carbonyl. The spectral region 10−70 ppm in Figure 2A, however, represents the carbons from terminal groups such as dimethylamino and the dodecyloxy unit. The core fragment is made up of 14 chemically different carbons, and therefore, 14 peaks (7 methine and 7 quaternary carbons) are noticed in Figure 2A. The chemical equivalency of an aromatic ring methine (ortho or meta carbon) is clear from the spectrum. The individual carbon numbers along with their chemical shift values are given in Table 1. In the case of terminal groups, the OCH_2 peak distinctly appears at 69.17 ppm and the peak at 40 ppm is assigned to dimethylamino carbons. The methyl carbon of the dodecyloxy chain is observed at 14 ppm, while the other carbons appear at 22−32 ppm.

^{13}C CPMAS on a Crystalline DoBDPMP. ^{13}C CPMAS experiments were performed on a crystalline powder of DoBDPMP at various temperatures. The spectral lines in the solid-state spectrum were assigned by comparison with the solution NMR data (Figure 2A) and with the help of commercial software.[15] The CPMAS spectrum of a crystalline DoBDPMP at room temperature obtained in a 400 MHz spectrometer is shown in Figure 2B. The spectrum in the region 100−165 ppm shows 21 peaks with varying intensity, in contrast to the solution NMR spectrum, where 14 signals were observed. The appearance of more signals in the region (100−165 ppm) for a solid is attributed to various phenyl ring orientations. To suppress the spinning sidebands in the CPMAS spectrum and to increase the resolution, a TOSS (total suppression of spinning sidebands) experiment was carried out with a 600 MHz spectrometer. The high-resolution CPMAS spectrum without spinning sidebands is given in Figure 3. It shows 25 well-resolved peaks in the chemical shift region 100−165 ppm (Figure 3), as compared to 21 peaks in the 400 MHz spectrum (Figure 2B). Close observation of the spectrum (Figure 3) revealed that the majority of additional peaks (10) appear in the region 110−135 ppm, which are mainly from the aromatic ring carbons (Table 1), while the region 145−165 ppm accounts for only 2 additional peaks. These additional peaks are attributed to different phenyl ring orientations of the core unit of the molecule. The TOSS

TABLE 1: Carbon-13 Chemical Shift Values (ppm) of DoBDPMP in Crystalline Solid, Nematic, and Isotropic Phases[a]

carbon number	23 °C solution (Figure 2A)	23 °C MAS (Figure 2B)	155 °C MAS (Figure 6B)	155 °C static (Figure 6C)	212 °C static (Figure 6D)
5	164.6	164.5	164.1	228.4	164.0
1	163.6	163.5	164.1	228.4	164.0
10	154.7	153.4	154.7	196.8	153.7
14	152.8	152.4	153.6	208.1	150.1
6	149.5	149.1	149.8	211.6	150.1
11	140.7	139.2	140.7	206.9	141.9
9	134.4	133.2	135.4	187.7	135.2
8	132.3	132.8	132.6	165.1	132.2
3	129.4	128.9	129.7	161.7	129.4
7	122.2	122.7	123.0	152.9	122.5
12	122.0	122.0	122.3	148.1	121.8
4	121.3				
2	114.3	114.2	115.1	142.5	115.2
13	112.8	111.9	113.4	137.1	113.6
B	68.3	69.0	69.1	63.8	69.2
A	40.7	40.2	40.7	45.1	40.5
C	31.9	32.7	32.5	25.1	31.9
D	29.6	32.0	30.2	25.1	29.6
E	29.6	32.0	30.2	25.1	29.6
F	29.6	32.0	30.2	25.1	29.6
G	29.3	32.0	30.2	25.1	29.6
H	29.3	31.2	30.2	25.1	29.6
I	29.0	31.2	30.2	25.1	29.6
J	25.9	26.7	26.6	25.1	26.2
K	25.9	26.7	26.6	25.1	26.2
L	22.6	23.4	23.0	22.1	22.5
M	14.1	15.5	14.3	13.6	13.8

[a] The quaternary C4 peak was only observed in solution and not in the solid state.

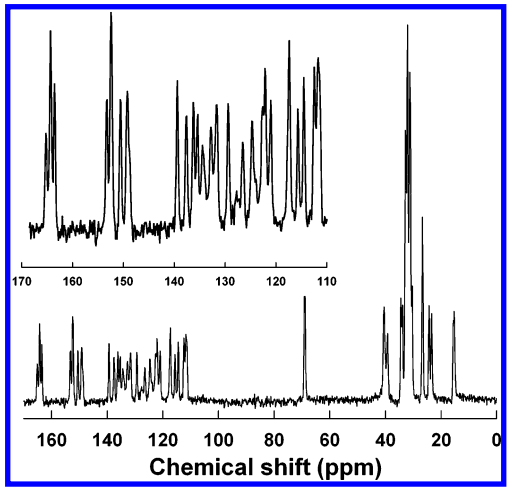

Figure 3. Carbon-13 CPMAS spectrum of DoBDPMP obtained under 6 kHz MAS using the TOSS technique to suppress the spinning sidebands at 23 °C.

spectrum also showed few additional peaks in the region 10−70 ppm, and among them, a peak at 40.37 ppm is notable.

To further assign the CPMAS data, two-dimensional chemical shift correlation of ^{1}H and ^{13}C nuclei using a HETCOR pulse sequence and ^{1}H CRAMPS experiments were carried out on a 600 MHz spectrometer. The ^{1}H CRAMPS spectrum in Figure 4 shows peaks from aromatic and azomethine protons in the region 6.7−8.5 ppm and aliphatic protons from terminal chains at 0.9−3.3 ppm. The peak intensity pattern is consistent with the number of aromatic and aliphatic protons. Further assignment of the CRAMPS spectrum is difficult due to the residual broadening, which could be due to the residual ^{1}H−^{1}H dipolar couplings and heterogeneous conformation of the molecule in the solid state. A 2D ^{1}H−^{13}C HETCOR spectrum of the solid

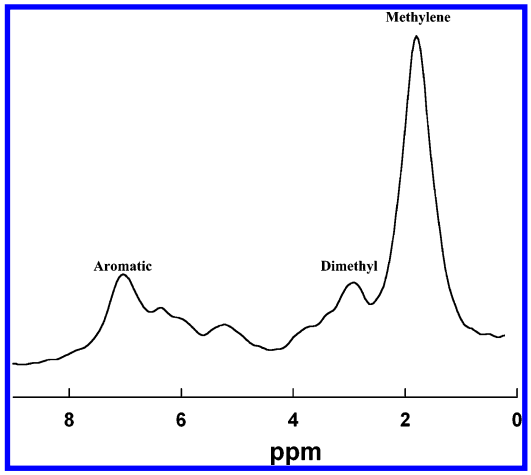

Figure 4. ^{1}H CRAMPS spectrum of DoBDPMP at 23 °C. A spinning speed of 5 kHz was used.

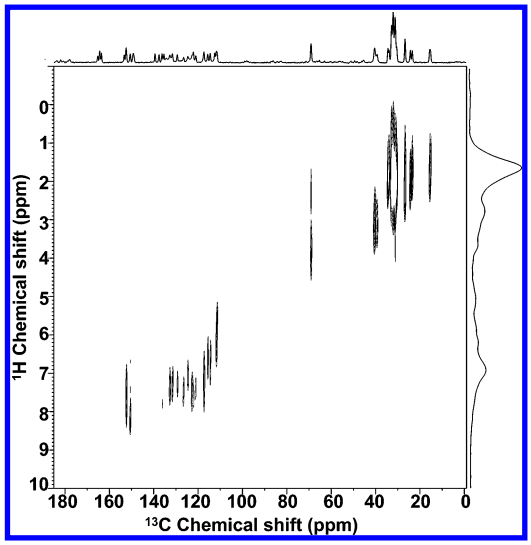

Figure 5. 2D ^{1}H−^{13}C HETCOR spectrum that correlates the isotropic chemical shifts of ^{1}H and ^{13}C nuclei of DoBDPMP at 23 °C. A spinning speed of 10 kHz was used.

is given in Figure 5. The absence of peaks for the quaternary carbons (C1, C4, C5, C6, C9, C11, and C14) in Figure 5 confirmed their assignment from the 1D CPMAS spectra (Figures 2B and 3), and it further increased the spectral resolution. The contour peaks observed in the region 110−165 ppm of the 2D spectrum also support the CPMAS data in Figure 2B. As many as 13 cross-peaks in the region 110−165 ppm are seen in the HETCOR spectrum, while there are only 7 chemically nonequivalent methine carbons in the molecule (6 from 3 phenyl rings and 1 from azomethine).

To examine the influence of temperature on a crystalline solid, a ^{13}C CPMAS experiment was carried out at 100 °C (well below T_{CN}), and the spectrum is given in Figure 2C. Interestingly, the region 110−165 ppm of the spectrum now accounts for fewer peaks than the room-temperature spectrum (Figure 2B). When the sample was cooled to room temperature, the reappearance of additional peaks was noted. This indicates the onset of phenyl ring reorientations at 100 °C. It is known that the molecular crystals undergo two types of changes with temperature: (a) phase transitions associated with rotational motions at a temperature below the melting point and (b) rotational motions associated with the melting transition.[32] The variable-temperature study of DoBDPMP below 146 °C (that is, T_{CN}) suggests that the disappearance of peaks in the ^{13}C chemical shift spectrum given in Figure 2C (compare the spectra in parts B

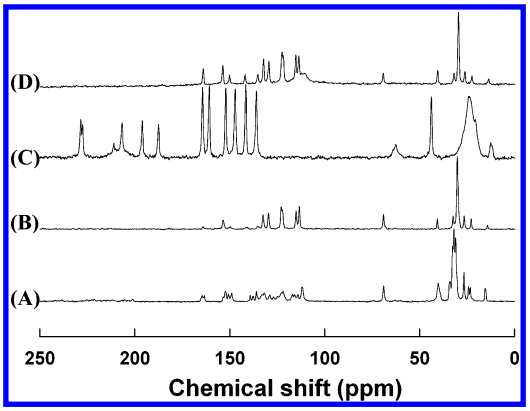

Figure 6. Carbon-13 chemical shift spectra of DoBDPMP: (A) 9 kHz MAS at 23 °C; (B) 6 kHz MAS at 155 °C; (C) under static conditions at 155 °C; (D) static spectrum obtained without cross-polarization at 212 °C. Spectra A, B, C, and D were obtained using 2020, 924, 560, and 376 scans, respectively.

and C of Figure 2) could be attributed to the above-mentioned condition a. It should be noted that the differential scanning calorimetry experiments did not show any peaks characteristic of crystal−crystal transitions.[15]

^{13}C CPMAS on a Nematic DoBDPMP. The ^{13}C CPMAS spectra of DoBDPMP in the crystalline (room temperature) and nematic (at 155 °C) phases are shown in parts A and B, respectively, of Figure 6; the chemical shift values are given in Table 1. The nematic-phase CPMAS spectrum (Figure 6B) shows 11 lines accounting for 14 different carbons in the region 100−165 ppm, and 7 signals are noticed in the region 10−70 ppm for 14 carbons (Table 1). Some of the peaks appearing in the region 110−165 ppm are sharp and intense and are mainly from ortho and meta methine carbons of the three phenyl rings and an azomethine carbon. However, the quaternary carbons appear as broad and low-intensity peaks. The signal at 164.1 ppm accounts for both the ester carbonyl carbon (C5) and the quaternary carbon (C1) of the phenyl ring adjacent to the oxymethylene carbon in the terminal dodecyloxy unit. The decrease in the number of peaks in contrast to that of the crystalline solid CPMAS spectrum is attributed to the fast rotational motions of phenyl rings that are characteristic of the nematic phase. The dimethylamino carbons in this spectrum show a single peak at 40.8 ppm. The isotropic chemical shift values from the spectra given in Figures 2A and 6B are similar (Table 1) and are also similar to those of the ^{13}C spectrum of the isotropic phase (212 °C) obtained without cross-polarization.

Static ^{13}C Spectrum of DoBDPMP in the Nematic Phase. Liquid crystals align in the presence of an external magnetic field. The orientation of the nematogen can be parallel or perpendicular and depends on the anisotropic magnetic susceptibility tensor.[33] However, the uniaxial nematic liquid crystals containing phenyl rings are known to orient with the molecular axis parallel to the magnetic field. For such macroscopically oriented molecules such as liquid crystals, MAS is not required to get high spectral resolution. The static ^{13}C spectrum of the compound in the nematic phase (at 155 °C) is shown in Figure 6C. The chemical shift values are distinctly different from those of the CPMAS spectra (Figure 6A,B). The appearance of well-spread-out narrow spectral lines in the nematic phase suggests the homogeneous alignment of molecules in the external magnetic field. The director is parallel to the magnetic field as the phase is uniaxial. The spectrum shows 12 peaks in the region 130−230 ppm and 4 peaks in the region 10−70 ppm (Table 1). The precise assignment of the chemical shift values in the nematic phase is difficult as the chemical shift anisotropy tensor

TABLE 2: Alignment-Induced Chemical Shift Values (ppm) of Different Carbons of DoBDPMP

carbon number	155 °C	170 °C	185 °C	200 °C
2	27.3	25.8	23.6	20.3
12	25.7	24.4	22.5	19.6
7	29.9	28.3	25.9	22.1
13	23.6	22.6	21.0	18.5
3	31.9	30.4	27.9	24.1
8	32.5	30.6	27.8	23.7
10	42.0	39.8	36.4	33.5
14	55.2	53.7	49.22	42.9
11	66.2	62.5	56.97	53.6
9	53.3	50.0	44.62	36.3
6	62.0	58.9	53.65	48.3
5	63.8	60.0	54.28	46.1
1	64.8	61.0	55.29	47.2

values of liquid crystals are not available in the literature. However, a tentative assignment can be carried out using the intensity pattern of the signals and by comparing the chemical shift values of structurally similar liquid crystals reported in the literature. Such an approach is commonly employed in the interpretation of spectra of oriented liquid crystals.[23,34] The spectrum in Figure 6C shows six sharp and very intense peaks in the region 130−170 ppm that are attributed to the methine carbons of the three phenyl rings. In the present work, the individual assignment of chemical shift values of the methine carbons of the three phenyl rings was carried out by comparison with the chemical shift values of 4-butoxybenzoic acid and 4-(((dodecyloxy)benzoyl)oxy)benzaldeyde, which represents ring I and ring II of the core fragment of DoBDPMP. The ortho and meta methine carbon chemical shift values of these compounds are used to identify the chemical shift values of the C2, C3 and C7, C8 carbons of DoBDPMP (Figure 6C). The appearance of one peak each for ortho and meta methine carbons of the phenyl rings of the core fragment is attributed to the fast rotation of the phenyl ring with respect to the para axis. Molecules in the nematic phase undergo rapid reorientation about the molecular axis, while the phenyl rings undergo π flips along the para axis.[26] The large span of the chemical shift tensors of aromatic,[35] carbonyl, and CH═N carbons provides a large dispersion of the peaks in this region of the spectrum. The alignment-induced chemical shift values of the core fragment carbons ($\delta_{lc} - \delta_{iso}$) are given in Table 2. The examination of these values indicates that the nonprotonated carbons show higher deshielding than the protonated carbons. A recent study attributed the extent of alignment-induced chemical shift values of protonated and nonprotonated carbons to their chemical shift anisotropic tensor values.[23] The high deshielding of nonprotonated carbons suggests their proximity to the molecular axis. Among the nonprotonated carbons, six are from three phenyl rings that are part of the para axes. The other nonprotonated carbon is part of the ester carbonyl linking unit. Since the para axes are close to the molecular axis, the nonprotonated carbons are deshielded.[23] Broad lines observed in the region 10−70 ppm (except the one for dimethyl carbons) are mainly due to the overlap of the signals from all the methylene carbons that have similar (but not identical) orientations with respect to the magnetic field. In addition, the narrow chemical shift span for the methylene carbons does not favor resolution of the peaks corresponding to different methylene carbon sites. The narrow line observed for methyl carbons of the dimethylamino at 43.9 ppm, in contrast to other carbons of the terminal units, is due to the rotation of the methyl group.

Since the static spectrum at 155 °C (Figure 6C) showed chemical shift values different from those of the CPMAS spectra

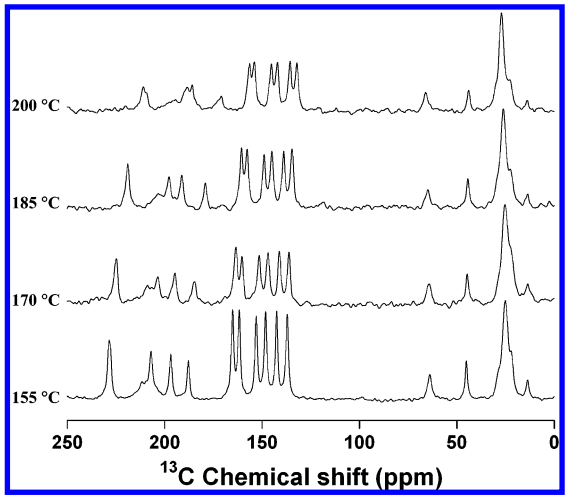

Figure 7. Static ^{13}C chemical shift spectra of DoBDPMP in the nematic phase obtained at various temperatures: (A) 155 °C; (B) 170 °C; (C) 185 °C; (D) 200 °C. Spectra A, B, C, and D were obtained using 280, 64, 64, and 64 scans, respectively.

TABLE 3: Carbon-13 Chemical Shift Values (ppm) (Figure 7) of DoBDPMP in the Nematic Phase at Various Temperatures

carbon number	155 °C	170 °C	185 °C	200 °C
5	228.4	224.6	218.9	210.8
1	228.4	224.6	218.9	209.3
10	196.8	194.5	191.1	188.3
14	208.1	206.5	202.0	195.7
6	211.6	208.5	203.2	197.8
11	206.9	203.3	197.7	194.3
9	187.7	184.4	179.0	170.8
8	165.1	163.3	160.5	156.3
3	161.7	160.1	157.6	153.8
7	152.9	151.3	148.9	145.1
12	148.1	146.8	144.9	142.0
4				
2	142.5	141.0	138.8	135.5
13	137.1	136.1	134.5	132.0
B	63.8	64.4	64.8	65.9
A	45.1	44.7	44.3	43.8
C−K	25.1	25.4	26.1	27.0
L	22.1	22.4	22.5	22.7
M	13.6	13.6	13.6	13.8

(Figure 6A,B) due to alignment, static experiments at 170, 185, and 200 °C were carried out to examine the variation of the chemical shift values. The static spectra of DoBDPMP are shown in Figure 7, and Table 3 gives the chemical shift values of all the carbons of the molecule. With increasing temperature, the chemical shift values approach the isotropic values, which clearly supports the decreasing molecular order in the magnetic field (Figure 8). The isotropic tumblings of molecules abruptly change the observed chemical shift values at the isotropic temperature (Figure 8). This is further confirmed by measuring the static spectrum at 212 °C (above the clearing temperature).

2D PITANSEMA. A combination of ^{13}C chemical shifts and ^{1}H−^{13}C dipolar couplings measured in the nematic phase will be highly valuable in determining the order parameter of different chemical groups of the molecule. Due to the magnetic alignment of liquid crystalline molecules in the nematic phase, the ^{1}H−^{13}C dipolar splittings do not disappear, while they are motionally averaged to zero by random tumbling in an isotropic phase. Typically, 2D separated-local-field (SLF) experiments are used to determine the heteronuclear dipolar couplings.[36] We recently demonstrated a new 2D pulse sequence, called PITANSEMA (polarization inversion time-averaged nutation spin exchange at the magic angle),[37,38] that uses a very low radio frequency power for the low gyromagnetic ratio unlike most other high-resolution SLF experiments. Since liquid crystalline materials are sensitive to the radio frequency heating, in this study, we measured the ^{1}H−^{13}C dipolar couplings at various temperatures using the 2D PITANSEMA method (Figure 9). The nematogen consists of seven CH carbons in the core fragment (six aromatic CH carbons and one azomethine CH carbon), and the measurement of ^{13}C−^{1}H dipolar couplings pertaining to these CH groups, which are sensitive to the orientation of the molecule, would not only support the assignment of chemical shift values from the 1D static measurement but also provide information about the molecular ordering. Further, the orientation of the mesogen in the magnetic field is mainly dictated by the core fragment, and therefore, the measurement of C−H dipolar couplings would facilitate the determination of molecular ordering. Figure 9 shows the 2D PITANSEMA spectra of the core fragment of the nematogen at different temperatures along with representative 1D dipolar coupling spectral slices of all CH carbons (six aromatic carbons and one azomethine carbon). The appearance of seven doublets with different chemical shift values in the spectrum clearly supports the assignment of ortho/meta carbons of three 1,4-disubstituted phenyl rings and azomethine in the mesogen. The C−H dipolar coupling values after scaling (a scaling factor 0.6 was used for the PITANSEMA sequence[37]) are given in Table 4. A close examination of the data given in Table 4 indicates the decrease in the dipolar coupling values with increasing temperature for all the carbons due to the increasing disorder of the molecule. This observation is consistent with the static 1D ^{13}C measurements at different temperatures where a decrease in the chemical shift values is noted with an increase in the temperature (Figure 8). The PITANSEMA experiment also

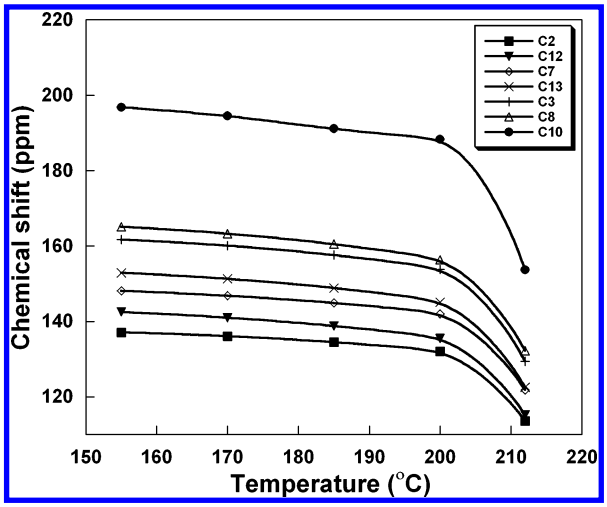

Figure 8. Temperature vs chemical shift values of the protonated carbons in the core fragment: C2 (filled squares), C12 (filled triangles), C7 (tilted squares), C13 (times signs), C3 (plus signs), C8 (triangles), and C10 (filled circles) of DoBDPMP.

TABLE 4: ^{13}C−^{1}H Dipolar Coupling Values (kHz) (from Figure 9) for the Core Fragment of DoBDPMP

carbon number	155 °C	170 °C	185 °C	200 °C
2	3.29	3.16	2.81	2.37
12	2.53	2.38	2.21	1.83
7	2.79	2.73	2.50	2.01
13	2.43	2.28	2.13	1.86
3	2.60	2.50	2.25	1.85
8	2.40	2.30	2.08	1.76
10	4.66	4.33	4.00	3.35

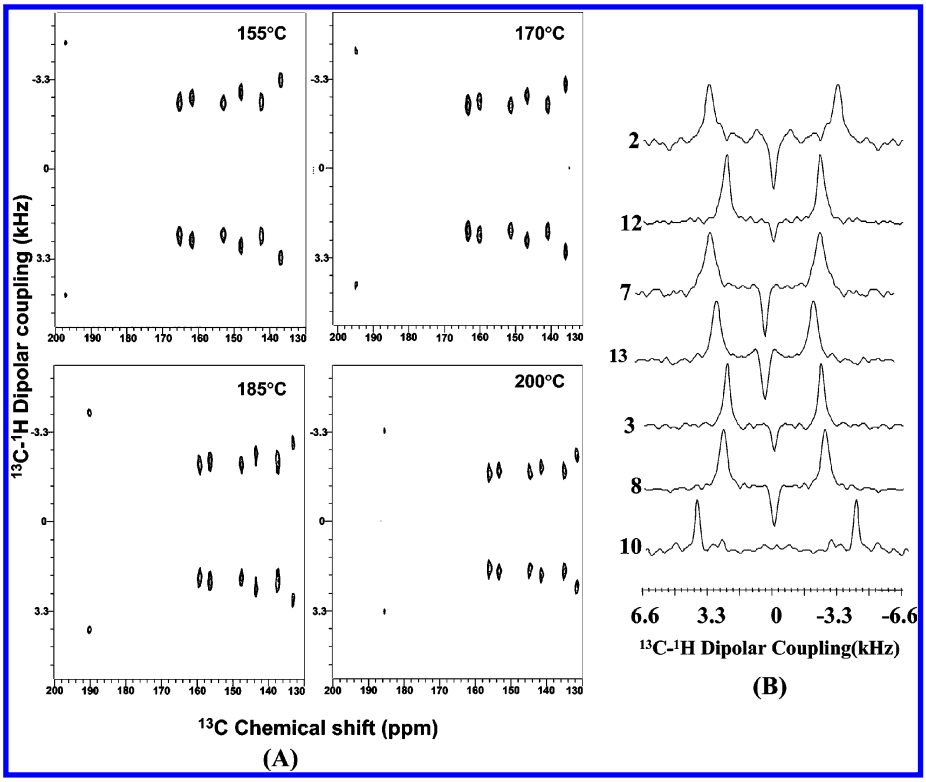

Figure 9. (A) 2D PITANSEMA spectra of DoBDPMP obtained at various temperatures. Note the decrease in the dipolar splitting with increasing temperature. The experimental parameters used to obtain this spectrum are $\tau_1 = 10$ μs, $\tau_2 = 5$ μs, 128 t_1 increments, 16 scans, and a 3 s recycle delay. (B) 1D ^{1}H−^{13}C dipolar coupling slices taken from the 2D spectrum at 185 °C.

supports the assignment of six phenyl ring CH carbons and an azomethine CH carbon of the core fragment.

Orientational Order Parameter. The determination of the orientational order of a mesogen in the magnetic field requires the ^{13}C−^{1}H dipolar coupling values and the direction of the molecular axis. The molecular axis (*M*) as shown in Figure 1 is assumed to pass through the centers of the phenyl rings. The deviation of the molecular axis from the para axes of the phenyl rings is attributed to the presence of the linking units. The support for this is readily seen from the dipolar coupling values of the C−H carbons of the phenyl rings (Table 4). The difference in the dipolar coupling values of the phenyl rings at any given temperature indicates the difference in their orientations. In the case of ring I, the variation of the C−H dipolar coupling is larger than that of rings II and III. This may be due to the different conformation of ring I, which is linked to ring II by a flexible ester unit, whereas rings II and III are linked through a more rigid azomethine group. A recent study reported smectic phases of a hockey stick shape mesogen that is structurally similar to DoBDPMP.[34] They noticed the influence of the conformation of ring I in the organization of molecules in a low-temperature smectic phase. Bayle and Fung[27] found a variation of the molecular axis within the mesogenic core from ring I and ring II in a four-unit-link-containing mesogen, and attributed the variation to the presence of a flexible ester link. Hence, in the present study, a 6° tilt of the molecular axis relative to the para axis of ring I was assumed while a 4° tilt was considered for rings II and III. Since the nematic phase is uniaxial and due to the cylindrical symmetry of the phase, the experimentally determined dipolar coupling values are related to the orientational order (*S*) by the following equation:

$$D = -S(h\gamma_C\gamma_H/4\pi^2 r_{CH}^3)(3\cos^2\theta - 1)/2$$

where *D* is the C−H dipolar coupling constant, *S* is the orientational order parameter, γ_i is the gyromagnetic ratio of nucleus *i*, r_{CH} is the distance between C and H nuclei, and θ is the angle between the C−H vector and the external magnetic field axis (or the molecular axis or the director). In view of the tilt of the molecular axis with respect to the para axes of phenyl rings, the following values for θ were used in determining the orientational order parameter values: 120° − 6° = 114° for ring I, 120° − 4° = 116° for rings II and III, and 114° − 4° = 110° for azomethine methine carbons.

TABLE 5: Orientational Order Parameters (*S*) of the Core Fragment of DoBDPMP

structural unit	155 °C	170 °C	185 °C	200 °C
ring I	0.51	0.49	0.44	0.36
ring II	0.54	0.52	0.47	0.39
ring III	0.51	0.48	0.45	0.38
link	0.63	0.58	0.54	0.45

The order parameter values for the azomethine link and three phenyl rings of DoBDPMP at different temperatures are given in Table 5. In this study, we assumed that the order parameter tensor is both axially symmetric and independent of any conformational changes in the molecule. The ratios of the order parameter for the linking unit (S_{link}) and the phenyl rings (S_{RII}) of the core unit are $S_{link}/S_{RI} = 1.21$, $S_{link}/S_{RII} = 1.13$, and $S_{link}/S_{RIII} = 1.20$. These values are linearly correlated and remain constant for a temperature range of 150−200 °C. A close examination of the *S* values of the three phenyl rings and their ratios with the linking unit reveals that rings I and III are less ordered than ring II. Similar trends are also reported in the NMR studies of thermotropic liquid crystals with two or more rings.[23−27] The variation of the order within the core of the mesogen is due to the difference in the linkage for each of the phenyl rings. In the case of DoBDPMP, one end of rings I and III is a flexible alkyl (alkoxy) unit whereas ring II experiences a different environment. The higher order parameter value for

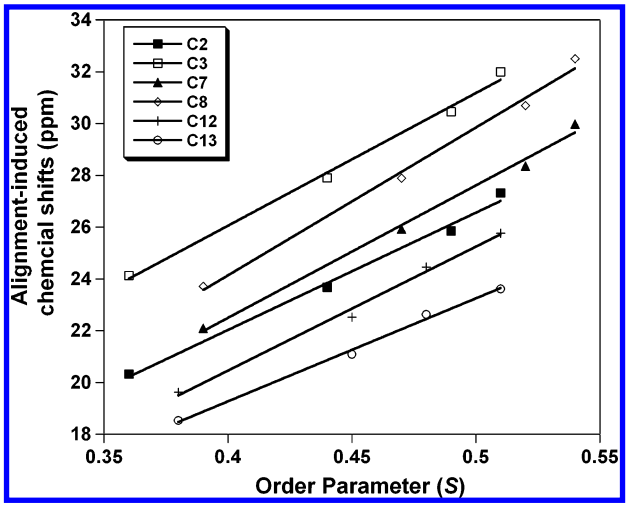

Figure 10. Orientational order and alignment-induced chemical shift values of protonated carbons of the phenyl rings of DoBDPMP: C2 (filled squares), C3 (squares), C7 (filled triangles), C8 (tilted squares), C12 (plus signs), C13 (circles).

the linking unit in contrast to the phenyl rings is due to the difference in its geometry and rigidity arising from the restricted rotation of the double bond. The NMR studies of MBBA and EBBA showed that the azomethine plane determines the overall orientation and ordering of the molecule in the magnetic field.[39,40] In the present case, the linking unit order can be viewed as a global order and the phenyl ring order as segmental. A plot of the order parameter of the phenyl rings and the alignment-induced chemical shift values at various temperatures shows linearity, thus supporting the validity of the molecular order (Figure 10). Similar trends have been reported for other liquid crystal molecules.[27,41] With an increase in temperature, the order parameter values decrease, indicating the increase in the fluctuations of the molecules.

Conclusions

Variable-temperature ^{13}C CPMAS NMR experiments of crystalline, meso, and isotropic phases of a novel nematogen (DoBDPMP) showed structural changes. The appearance of many additional peaks in the crystalline solid was attributed to different phenyl ring orientations that disappeared even before melting. The static spectrum of the compound in the nematic phase indicated the parallel alignment of the nematogen in the magnetic field. The rapid reorientation of phenyl rings was noticed from the chemical shift values of ortho/meta carbons. An increase in temperature resulted in a decrease in the chemical shift values of the molecule in the nematic phase. The variable-temperature static 2D PITANSEMA spectra provided the assignment of methine carbons of phenyl rings and azomethine and the dipolar coupling values which were used to determine the orientational order. The variation in the ordering of three phenyl rings and the linking unit of the core fragment is attributed to different substituents and their geometry. We believe that the solid-state NMR approach presented in this paper would be useful to study other types of liquid crystalline materials. For example, the relative orientation of different chemical groups can be measured in structurally complicated systems such as banana-type systems,[42] thiophene-based liquid crystals,[43−47] and metallomesogens.[48,49]

Acknowledgment. This research was supported by research funds to A.R. We thank Yamamoto and Ermakov for helpful discussions. T.N. is on a sabbatical leave from the Central Leather Research Institute, India.

References and Notes

(1) Kato, T. *Struct. Bonding (Berlin)* **2000**, *96*, 96.
(2) Beginn, U. *Prog. Polym. Sci.* **2003**, *28*, 1049.
(3) Percec, V.; Glodde, M.; Bera, T. K.; Miura, Y.; Shiyanovskaya, L.; Singer, K. D.; Balagurusamy, V. S. K.; Heiney, P. A.; Schnell, I.; Rapp, A.; Speiss, H. W.; Hudson, S. D.; Duan, H. *Nature* **2002**, *419*, 384. Freek J. M. H.; Jonkheijm, P.; Meijer, E. W.; Schenning, A. P. H. J. *Chem. Rev.* **2005**, *105*, 1491.
(4) Kouwer, P. H. J.; Jager, F. W.; Mijs, W. J.; Picken, S. J. *Macromolecules* **2002**, *35*, 4322.
(5) Ito, T.; Kato, A.; Kobinata, S. *Liq. Cryst.* **2001**, *28*, 89.
(6) Ostuni, E.; Weiss, R. G. *Liq. Cryst.* **1999**, *26*, 541.
(7) Fischbach, I.; Pakula, T.; Minkin, P.; Fechtenkotter, A.; Mu1llen, K.; Spiess, H. W. Saalwachter, K. *J. Phys. Chem. B* **2002**, *106*, 6408.
(8) Rappoport, D.; Furche, F. *J. Am. Chem. Soc.* **2004**, *126*, 1277.
(9) Jodicke, J. C.; Luthi, H. P. *J. Chem. Phys.* **2002**, *117*, 4146.
(10) Kohn, A.; Hattig, C. *J. Am. Chem. Soc.* **2004**, *126*, 7399.
(11) Wilson, J. N.; Bunz, U. H. F. *J. Am. Chem. Soc.* **2005**, 127, 4124.
(12) Kushto, G. P.; Jagodzinski, P. W. *J. Mol. Struct.* **2000**, *516*, 215.
(13) Coe, B. J.; Harris, J. A.; Brunschwig, B. S.; Garin, J.; Orduna, J. *J. Am. Chem. Soc.* **2005**, *127*, 3284.
(14) Coe, J. B.; Harris, J. A.; Asselberghs, I.; Wostyn, K.; Clays, K.; Gelbrich, T.; Light, M. E.; Hursthouse, M. B.; Nakatani, K. *Adv. Funct. Mater.* **2003**, *13*, 347.
(15) Narasimhaswamy, T.; Srinivasan, K. S. V. *Liq. Cryst.* **2004**, *31*, 1457.
(16) Luckhurst, G. R.; Gray, G. W. *The Molecular Physics of Liquid Crystals*; Academic Press: New York, 1979.
(17) Frisch, M. R.; Kumar, S. In *Liquid Crystals-Experimental Study of Physical Properties and Phase Transitions*; Kumar S., Ed.; Cambridge University Press: Cambridge, U.K., 2001; Chapter 1, p 1.
(18) Seed, A. J.; Toyne, K.; Goodby, J. W.; Hird, M. *J. Mater. Chem.* **1995**, *5*, 1. Beekmans, F.; Boer, P. D. *Macromolecules* **1996**, *29*, 8726. Chrzumnicka, E.; Szybowicz, M.; Bauman, D. *Z. Naturforsch., A: Phys. Sci.* **2004**, *59*, 510. Van Boxtel, M. C. W.; Wubbenhorst, M.; Vanturnhout, J.; Bastiaansen, C. W. M.; Broer, D. J. *Liq. Cryst.* **2003**, *30*, 235.
(19) *NMR of Ordered Liquids*; Burnell, E., De Lange, C. A., Eds.; Kluwer: Boston. 2003.
(20) Dvinskikh, V. S.; Zimmermann, H.; Maliniak, A.; Sandstrom, D. *J. Magn. Reson.* **2003**, *163*, 46.
(21) Zimmermann, H.; Bader, V.; Poupko, R.; Wachtel, E. J.; Luz, Z. *J. Am. Chem. Soc.* **2002**, *124*, 15286.
(22) Caldarelli, S.; Hong, M.; Emsley, L.; Pines, A. *J. Phys. Chem.* **1996**, *100*, 18696.
(23) Nakai, T.; Fujimori, H.; Kuwahara, D.; Miyajima, S. *J. Phys. Chem. B* **1999**, *103*, 417.
(24) Dong, R. Y.; Fodor-Csorba, K.; Xu, J.; Domeici, V.; Prampolini, G.; Veracini, C. A. *J. Phys. Chem. B* **2004**, *108*, 7694.
(25) Tan, C.; Fung, B. M. *J. Phys. Chem. B* **2003**, *107*, 5787.
(26) Fung, B. M. *Prog. Nucl. Magn. Reson. Spectrosc.* **2002**, *41*, 171.
(27) Bayle, J. P.; Fung, B. M. *Liq. Cryst.* **1993**, *15*, 87.
(28) Shekar, S. C.; Lee, D. K.; Ramamoorthy, A. *J. Magn. Reson.* **2002**, *157*, 223.
(29) Metz, G.; Wu, X.; Smith, S. O. *J. Magn. Reson., A* **1994**, *110*, 219.
(30) Bennett, A. E.; Rienstra, C. M.; Auger, M.; Lakshmi, K. V.; Griffin, R. G. *J. Chem. Phys.* **1995**, *103*, 6951.
(31) Praefcke, K.; Singer, D. In *Hand Book of Liquid Crystals*; Demus, D., Goodby, J., Gray, G. W., Spiess, H. W., Vill, V., Eds.; Wiley-VCH: Weinheim, Germany, 1998; Vol. 2B, p 945.
(32) *Liquid crystals*; Chandrasekhar, S., Ed.; Cambridge University Press: Cambridge, U.K., 1992; Chapter 2.1, p 17.
(33) Dong, R. Y. *Nuclear Magnetic Resonance of Liquid crystals*, 2nd ed.; Springer: New York, 1997; Chapter 1, p 1.
(34) Das, B.; Grande, S.; Weissflog, W.; Eremin, A.; Schroder, M. W.; Pelzl, G.; Diele, S.; Kresse, H. *Liq. Cryst.* **2003**, *30*, 529.
(35) Wei, Y.; Lee, D. K.; Ramamoorthy, A. *J. Am. Chem. Soc.* **2001**, *123*, 6118; Birn, J.; Poon, A.; Mao, Y.; Ramamoorthy, A. *J. Am. Chem. Soc.* **2004**, *126*, 8529.
(36) Ramamoorthy, A.; Wei, Y.; Lee, D. K. *Annu. Rep. NMR Spectrosc.* **2004**, *52*, 2.
(37) Lee, D. K.; Narasimhaswamy, T.; Ramamoorthy, A. *Chem. Phys. Lett.* **2004**, *399*, 359.
(38) Nishimura, K.; Naito, A. *Chem. Phys. Lett.* **2005**, *402*, 245−250.
(39) Hohener, A.; Muller, L.; Ernst, R. R. *Mol. Phys.* **1979**, *38*, 909.
(40) Nagaraja, C. S.; Ramanthan, K. V. *Liq. Cryst.* **1999**, *26*, 17.

(41) Guo, W.; Fung, B. M. *J. Chem. Phys.* **1991**, *95*, 3917.
(42) Xu, J.; Csorba, F.; Dong, R. Y. *J. Phys. Chem. A* **2005**, *109*, 1998.
(43) Nugent, S. J.; Wang, Q. M.; Bruce, D. W. *New. J. Chem*. **1996**, *20*, 669.
(44) Eichhorn, S. H.; Paraskos, A. J.; Kishikawa, K.; Swager, T. M. *J. Am. Chem. Soc*. **2002**, *124*, 12742.
(45) Narasimhaswamy, T.; Somanathan, N.; Lee, D. K.; Ramamoorthy, A. *Chem. Mater*. **2005**, *17*, 2013.
(46) Narasimhaswamy, T.; Lee, D. K.; Somanathan, N.; Ramamoorthy, A. *Chem. Mater*. **2005**, *17*, 4567.
(47) Narasimhaswamy, T.; Lee, D. K.; Yamamoto, K.; Somanathan, N.; Ramamoorthy, A. *J. Am. Chem. Soc.* **2005**, *127*, 6958.
(48) Bruce, D. *Acc. Chem. Res*. **2000**, *33*, 831.
(49) Morale, F.; Date, R. W.; Guillon, D.; Bruce, D. W.; Finn, R. L.; Wilson, C.; Blake, A. J.; Schroder, M.; Donnio, B. *Chem.—Eur. J.* **2003**, *9*, 2484.